

# Aeroponic systems design: considerations and challenges

Albert Min,<sup>1,2</sup> Nam Nguyen,<sup>1,2</sup> Liam Howatt,<sup>1,2</sup> Marlowe Tavares,<sup>1,2</sup> Jaho Seo<sup>1</sup>

<sup>1</sup>Department of Automotive and Mechatronics Engineering, Faculty of Engineering and Applied Science, Ontario Tech University, Oshawa; <sup>2</sup>PowerPlant Agriculture Inc., Calgary, AB, Canada

## Abstract

Controlled Environment Agriculture holds promise as a way to intensify current agricultural production systems while limiting pressures on land, water, and energy resources. However, its use has not yet been widely adopted, partly because the engineering design considerations and associated challenges are not well known. This is even more apparent for aeroponics, where the additional cost and complexities in controlling atomisation have yet to establish an advantage in scale over simpler hydroponic systems.

To shed light on these considerations and challenges, an instrumented aeroponic system was prototyped to create a quantitative growth model for various species of leafy greens. As the

first consideration, pressure swirl atomisers were paired with a diaphragm-type pressure tank to supply the necessary pressures needed for effective atomisation. Secondly, the nutrient solution was mixed on demand from Reverse Osmosis water, and the concentrated nutrient stock was then pumped into the pressure tank using a positive displacement pump. A bamboo-based substrate that allowed germination and extended vegetative growth was supported on a stainless-steel mesh and PVC frame acting as a grow tray. Finally, a camera microservice platform was developed using a computer vision pixel-based segmentation method to quantify plant growth.

Correspondence: Jaho Seo, Faculty of Engineering and Applied Science, Ontario Tech University, Oshawa, ON, Canada.  
E-mail: Jaho.Seo@ontariotechu.ca

Key words: controlled environment agriculture; aeroponics; vertical farming; atomising nozzles; fertigation; computer vision.

Acknowledgements: this study was supported by the Mitacs Research Training Award (Application Ref: IT20327).

Contributions: all authors have contributed equally.

Conflict of interest: the authors declare no potential conflict of interest.

Funding: none.

Availability of data and materials: data and materials are available by the authors.

See the online Appendix for additional Figures.

Received for publication: 19 February 2022.

Revision received: 28 June 2022.

Accepted for publication: 30 June 2022.

©Copyright: the Author(s), 2023

Licensee PAGEPress, Italy

Journal of Agricultural Engineering 2023; LIV:1387

doi:10.4081/jae.2022.1387

This article is distributed under the terms of the Creative Commons Attribution Noncommercial License (by-nc 4.0) which permits any non-commercial use, distribution, and reproduction in any medium, provided the original author(s) and source are credited.

Publisher's note: all claims expressed in this article are solely those of the authors and do not necessarily represent those of their affiliated organizations, or those of the publisher, the editors and the reviewers. Any product that may be evaluated in this article or claim that may be made by its manufacturer is not guaranteed or endorsed by the publisher.

## Introduction

Controlled Environment Agriculture (CEA) is a technology-based approach to intensifying food production systems. It is a continuation of what has been the trend in agriculture since its inception, greater monitoring and control over the physical, chemical, and biological environments involved in the health and growth of plants. This type of agriculture encompasses a variety of agricultural and general-purpose technologies such as indoor farming, LEDs, automation, and machine learning. Some benefits of coupling these innovations with farming include reduction of food miles, seasonal and geographic independence of food production, improved product consistency, isolation from pathogen pressures, utilisation of disused urban spaces, and price stabilisation (Despommier, 2011; Specht *et al.*, 2014; Benke *et al.*, 2017). In addition to these promises, global trends, and industry-specific change accelerators have spurred public interest and investment in CEA. Trends include growing population, increasing urbanisation, and climate change, while change accelerators include new consumer preferences, emerging technologies, and reconfiguration of supply chains (Laugerette and Stöckel, 2016).

Hydroponics is a technology in the CEA portfolio related to growing plants in a water-based, nutrient-rich solution. It uses a soilless substrate to fix the plants in a cultivation unit, which exposes plant shoots to the air and plant roots to the nutrient solution. Irrigation methods to water and fertilise plants include the Nutrient Film Technique, Deep Water Culture, ebb and flow, drip, and aeroponic systems (Kozai, 2018). The realised benefits of hydroponics include improving water use efficiency and reducing eutrophication. Of the multitude of hydroponic systems, aeroponics claims to offer greater productivity due to the superior access that roots have to oxygen (Li *et al.*, 2018; Thakur *et al.*, 2019). In aeroponics, nutrient-rich droplets are periodically generated and deposited onto hanging plant roots. Because the roots are suspended in air, root aeration is enhanced as oxygen demand can be met by exchange and transport in the gas phase.

In comparison, oxygen exchange between tissues immersed in water and the aqueous environment is strongly impeded (Colmer, 2003). O<sub>2</sub> diffusivity in water is approximately 10,000 times slower

than in gaseous environments due to the increased collision of Oxygen molecules with water, resulting in a shorter mean free path (Pittman, 2016). In addition, the dissolved oxygen concentration in water is orders of magnitude lower than the concentration of oxygen gas in the atmosphere. Room temperature water at 100% O<sub>2</sub> saturation has an oxygen concentration of approximately 9 ppm, whereas the oxygen concentration in the atmosphere is 209,460 ppm. Many articles discuss these supposed differences between aeroponic, hydroponic, and soil-grown plants (Li *et al.*, 2018; Thakur *et al.*, 2019). Some points of comparison include biomass morphology (*i.e.*, leaf height, number of leaves), physiological markers (*i.e.*, photosynthetic rate, stomatal conductance), and metabolite content (*i.e.*, phenolic content, flavonoids). However, few go into detail on the design of the growing system being used beyond a parts list. This not only makes a comparison of findings difficult but also poses challenges to reproducibility. Furthermore, if system configuration is believed to be a contributing factor to the points of comparison, this will act as a confounding variable between studies. This paper presents the design process and learning lessons of our pressure atomiser aeroponic system with a drain-to-waste operation and a direct seed-to-harvest (no transplant) growth cycle. The study's objective was to design and prototype an instrumented aeroponic unit capable of creating a quantitative model of plant growth for various species of leafy greens. To achieve this, the atomisation system, fertiliser dosing unit, grow tray and substrate, and growth monitoring hardware and algorithms were designed as key subsystems for the developed prototype.

## Materials and Methods

The aeroponic system consists of a fertiliser dosing unit, an atomisation system located within two root chambers, broad-spectrum LED fixtures, and hardware to automate tasks and collect data (Appendix Figures 1 and 2). The design intent of the two root chambers was to have independent control of irrigation, nutrients, and lighting. Although it increased cost, the ability to run concurrent experiments and the subsequent reduction in total experiment time was thought to be a worthwhile trade-off.

The fertiliser dosing unit mixes Reverse Osmosis (RO) water and concentrated nutrient stock to make a diluted nutrient solution. This nutrient solution is pumped inside a pressure tank and kept under pressure. The pressurized solution is discharged through multiple atomizers onto plant roots. Solenoid valves control the spray cycle by regulating the solution flow between the pressure tank and atomisers. Plants are seeded and grown on a bamboo-based substrate supported by a grow tray. The grow tray height can be adjusted manually based on the root architecture of the plant. Multiple sensors measure parameters related to the nutrient solution, radiation, and the climate at the canopy and inside the root chamber. In addition, a vision system with cameras collecting colour images is used to monitor the growth status of leafy greens. Detailed descriptions of each subsystem are provided in the next section.

### Atomisation

Atomisation is a process where a bulk liquid is converted into small droplets. It is achieved by disrupting the consolidating influence of surface tension by various internal and external forces (Lefebvre and McDonell, 2017). Many sources in academia and popular literature consider the degree of atomisation as an important parameter in aeroponics and commonly reference an ideal

droplet diameter between 30 – 100  $\mu\text{m}$  (Lakhiar *et al.*, 2018). Larger droplets lead to less oxygen being available in the root system, whereas smaller droplets produce excessive root hair growth. These findings, however, are originally from a NASA-sponsored study conducted in microgravity, where different forces dominate fluid effects (Clawson *et al.*, 2000).

Nevertheless, the authors suggest that similar mechanics are at play in terrestrial applications. They state that a root's mist collection efficiency depends on its filament size as well as the droplet's size and velocity. For example, a 1  $\mu\text{m}$  droplet with a velocity of 30 m/s will impinge and collect on a 25  $\mu\text{m}$  wire, but not on larger diameter structures and not at lower velocities. As such, 1  $\mu\text{m}$  droplets are suspected to be too small for aeroponics as the necessary impingement velocities would take too much energy and possibly disturb root growth (Clawson *et al.*, 2000). On the other hand, 100  $\mu\text{m}$  droplets will fall too rapidly out of the air stream. This suspected minimum droplet size agrees with terrestrial mist deposition experiments performed on hairy root cultures of *Artemisia annua* (Wyslouzil *et al.*, 1997). They found that deposition efficiency curves as a function of droplet diameter have a sigmoidal shape with very few 1–2  $\mu\text{m}$  droplets depositing, followed by a sharp increase in efficiency for larger particle sizes.

Beyond deposition, a complete model for an aeroponic irrigation cycle has been proposed by Eldridge *et al.* (2020). They reason that the deposited droplets coalesce to form a thin, nutrient-dense aqueous film. The root surface retains these films over a period of time before decaying due to the effects of evaporation and gravity. This 3-stage process of deposition, retention, and decay is reasoned to be dynamic and exhibits spatiotemporal heterogeneity based on droplet composition, plant root architecture, and environmental properties. With this information, we can now describe the selection and design of the atomisation system. The system requirements are: i) generate droplets larger than 1  $\mu\text{m}$  but smaller than 100  $\mu\text{m}$ ; ii) provide uniform coverage throughout the entire root chamber volume; iii) enable a control regime that accommodates the changing fertigation and oxygen demands at various developmental stages of the plant.

The first requirement can be met by various types of atomisers, each with different working principles (Lefebvre and McDonell, 2017). Atomisers currently being used in aeroponics include pressure, air-assist, and ultrasonic atomisers. Pressure atomisers operate by discharging the liquid through a small orifice, converting pressure into kinetic energy. The resultant jet or sheet that's formed eventually breaks up into droplets as the kinetic energy overcomes the surface tension of the liquid. Air-assist atomisers expose liquid to a stream of high-velocity air. This liquid-gas interaction at high relative velocities causes a breakup of the liquid. Finally, ultrasonic atomisers feed liquid over a transducer and horn, which vibrates at ultrasonic frequencies to produce the short wavelengths necessary for fine atomisation. These 3 atomisers require different supporting systems and pose the greatest knock-on impact on the rest of the growing unit as well as requirements 2 and 3. Table 1 shows the comparison of these 3 types of atomisers.

With the goal of maximising potential scale and reliability, pressure atomisers were chosen due to their simplicity of operation. With all 3 technologies, it can be reasonably assumed that multiple atomisers would be needed to service the unit. In such a distributed atomisation system, pressure atomisers only require nutrient solution at the point of atomisation, whereas air-assist and ultrasonic atomisers also require compressed gas and electricity, respectively. Should air-assist atomisers be chosen, a compressed gas subsystem would need to be designed and integrated into the unit, including air compressors, air tanks, pneumatic valves, and a

way to distribute this gas to every nozzle. Ultrasonic atomisers can leverage existing electrical infrastructure, but care must be taken to avoid water ingress in electronics so close to the point of atomisation. Although there are many manufacturers of pressure atomisers, few provide detailed technical information to enable direct comparison. In an ideal world, the mean droplet diameter, droplet size distribution, patternation, spray angle, and flow rate would all be provided as a function of supply pressure. Nonetheless, 4 manufacturers of pressure atomisers with sufficiently detailed datasheets were identified and listed in Table 2. These are Pentair, TeeJet, BETE, and Ikeuchi. As nozzle size shows an inverse relation to atomisation quality, only the lowest flow rate variants were chosen for comparison (Lefebvre and McDonell, 2017).

The main difference between the 4 nozzles is their physical connection. Except for the TeeJet TX-VS1, all require a female thread on the liquid distribution. Using PVC pipes, these female threads can either be cut directly into the pipe wall, or a tee fitting can be used at every nozzle. The first option may seem lower in cost, but the size of pipe required to satisfy the effective thread engagement length quickly negated the cost advantage and was additionally deemed too large to package. For 1/8 NPT and 1/4 NPT, the required schedule 80 PVC pipe sizes to satisfy thread engagement lengths of 6.70 mm and 10.21 mm are 2½ and 6, respectively. The second option of using tee fittings at every nozzle was deemed too expensive of a manufacturing process for a scalable system. For every nozzle in the system, the distribution pipe would need to be cut to length and cemented onto a tee joint with threaded reducing adapters. The TX-VS1, on the other hand, only requires an unthreaded hole to be drilled on the pipe wall. Although it requires an assembly consisting of a nozzle body,

strainer, and cap for operation, this was considered an advantage as it did not depend on craftsmanship, as with cutting and cementing. The nozzle body can also be configured with a ball or a diaphragm check valve, with the latter coming in a slightly larger form factor. This enabled an investigation of the effects of a check valve on transient nozzle performance during the start and end of a spray cycle. The transient performance was deemed to be important as short spray durations were targeted for the study, the rationale for which is explained later in the paper. Under these justifications, the TX-VS1 was chosen over the other alternatives. The assemblies are shown in Figure 1.





The second requirement of uniform spray coverage throughout the root chamber was admittedly poorly satisfied. Although the requirement itself is well defined, spray coverage and its influencing parameters were difficult to determine either analytically or experimentally. For any given count, location, and orientation of nozzles, a spray distribution exists along the X (length), Y (width), and Z (depth) axes of the root chamber. For the TX-VS1 and other pressure atomisers, the spray takes on a hollow cone pattern with a ring-shaped impact area, as shown in Figure 2.

The difficulty lies in quantitatively assessing these measures of spray uniformity. Experimental tools to quantify spray patterns include mechanical and optical patternators (Lefebvre and McDonell, 2017). However, the former requires a downward spray direction, whereas the latter is cost-prohibitive. The upward spray direction of this application is particularly challenging to design as the initial spray pattern formation may not reflect actual spray coverage once the flow becomes turbulent and spreads inside the root chamber. Moreover, even if all spray characteristics were known to perfect detail, plant roots can both adapt and alter this

**Table 1. Comparison matrix of 3 different atomiser types: droplet size distributions show typical performance in each category.**

	Pressure	Air-assist	Ultrasonic
Requirements at the point of atomisation	Liquid (high pressure)	Liquid (low pressure/standing) Gas (variable pressure)	Liquid (low pressure/standing) Electricity
Mean droplet diameter between 1–100 µm	Yes	Yes	Yes
Droplet size distribution	Polydisperse	Polydisperse	Monodisperse

**Table 2. Comparison matrix of the lowest flow rate atomising nozzles from 4 different manufacturers.**

				
	Pentair – CS301AFD0.7-80 (Pentair, 2018)	TeeJet – TX-VS1 (TeeJet, 2014)	BETE – UML63M (BETE, 2019)	Ikeuchi – 1/4M KB 80 063N S303 (IKEUCHI)
Mean droplet diameter (µm)	61–105	61–105	<60	35
Operating pressure range (bar)	3–10	2–20	3–69	5–70
Flow rate (LPH)	2.76–5.05	3.30–8.58	2.38–12.11	1.13–5.58
Spry angle (deg)	80	80	80	80
Physical connection	1/8 MNPT	Nozzle body	1/8 MNPT	1/4 MNPT

MNPT, male national pipe thread.

environment. Despite these unknown nozzle parameters and complex root-environment interaction effects, the decision was made to optimize the coverage with respect to the uppermost grow tray plane using a simple geometric spray model. This plane was chosen to ensure germinating seeds could be kept moist throughout the entire grow tray. To cover the centre of each hollow cone ring while minimising spray overlap, the spray patterns of adjacent nozzles

were located to intersect this centre. The simplified model assumes that gravity does not affect spray patterns and travel in straight-line paths. Root chamber volumes outside the initial spray formation were assumed to be covered by the turbulent breakup of sprays. The dimensional parameters used in the development of the nozzle array are listed in Table 3 and shown in Figure 3. These geometries were designed in a 3D modelling application.

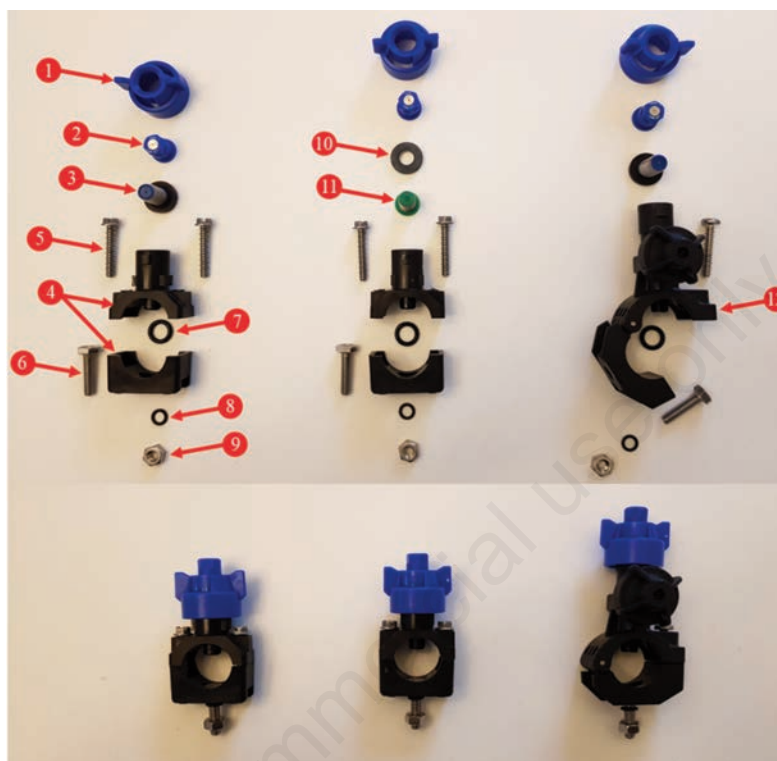


Figure 1. Exploded and assembled views of the TX-VS1 nozzle assemblies: among the 3 tested check valve configurations, the left assembly has no check valve, the middle assembly has a 10 psi Ball Check Valve, the right assembly has a 10 psi Diaphragm Check Valve. 1, cap; 2, nozzle; 3, strainer, integrated gasket; 4, nozzle body parts; 5, self tapping screw, clamps nozzle bodies; 6, bolt, fastens nozzle body to floor; 7, O-ring, nozzle body shank – pipe; 8, O-ring, nozzle body – floor; 9, nut; 10, gasket, cap; 11, strainer, 10psi ball check valve; 12, nozzle body, 10 psi diaphragm check valve.

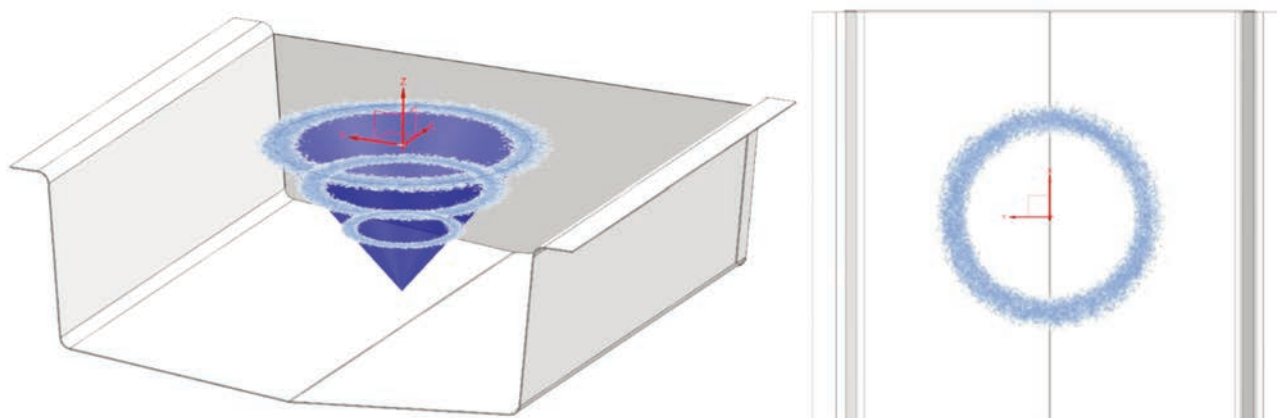


Figure 2. The initial spray pattern formation of a single generic hollow cone nozzle.

Multiple piping configurations can be used to feed this nozzle array with nutrient solution. The main point of comparison was the ratio of solenoid valves to nozzles. A 1:1 ratio allows independent control of nozzles at the expense of cost. Greater independent control was thought to be desirable as it reduces intersecting spray patterns. Colliding droplets can sometimes coalesce to increase the average size of particles in the spray. In addition to the ratio, the solenoid valves control the spray duration and frequency of the nozzle array, satisfying the final requirement. With this in mind, a counter parallel pipe system with a valve-to-nozzle ratio of 1:8 was chosen, as seen in Figure 4.

### Fertiliser dosing unit

The fertiliser dosing unit is responsible for mixing, storing, and delivering the diluted nutrient solution to the TeeJet TX-VS1 pressure swirl nozzles. The main knock-on effect of using these nozzles is the high supply pressures needed for atomisation. An increase in supply pressure causes the liquid to be discharged from

the nozzle at a higher velocity, which promotes a finer spray (Lefebvre and McDonell, 2017). In addition, there are 2 growing zones where nutrient concentrations need to be adjusted independently of one another. With the above information, we can now describe the design of the fertiliser dosing unit. The system requirements are: i) deliver the diluted nutrient solution to nozzles at up to 10 bar supply pressures; ii) achieve independent control of nutrient concentrations between the 2 root chambers; iii) enable a control regime that accommodates the changing water and nutrient demands at various developmental stages of the plant.

The first requirement can be met using various process-control devices such as Positive Displacement (PD) pumps, centrifugal pumps, and pressure tanks. Although there are many subclassifications within PD and centrifugal pumps, the primary difference lies in their performance curves. While PD pumps produce relatively constant flow rates throughout their discharge pressure range, centrifugal pumps produce variable flow rates. The intersection of these pump curves with the system resistance curve determines the pump's operating point, as shown in Figure 5.

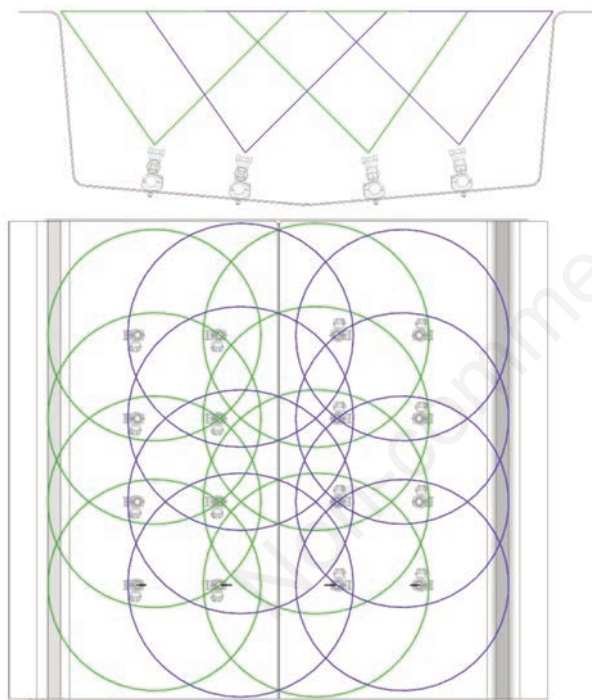


Figure 3. Nozzle array pattern in the YZ (upper) and XY (lower) plane.

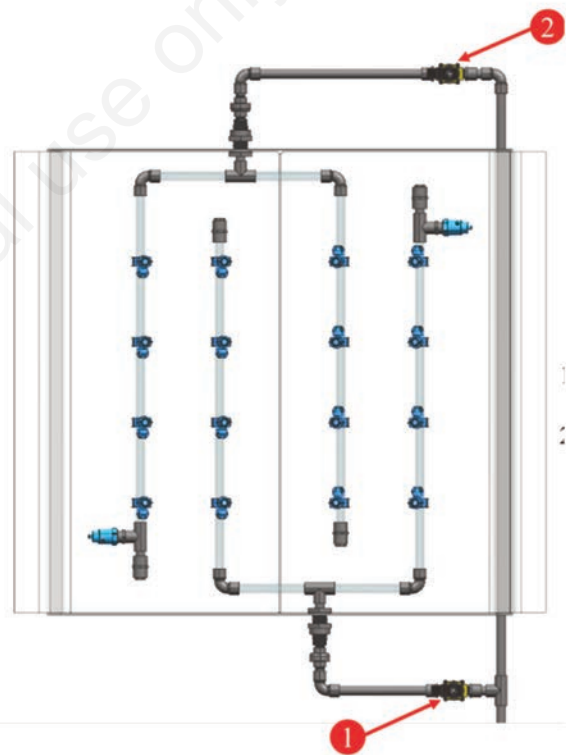


Figure 4. Final nozzle array configuration. 1, diaphragm type solenoid valve, boom 1; 2, diaphragm type solenoid valve, boom 2.

Table 3. Relevant dimensional parameters to the design of the nozzle array.

Dimensional Parameter	Value	Comments
Grow tray plane, length x width	1.22x1.22m	Matched to the coverage of LED fixtures
Nozzle, floor-to-tip length (DCV variant)	110mm	Manufacturer specifications
Nozzle, spray angle	80 degrees	Manufacturer specifications
Root chamber, drain angle	5 degrees	Design value
Inner nozzles, distance from root chamber centre (along the floor)	155mm	Design value
Outer nozzles, distance from root chamber centre (along the floor)	365mm	Design value

DCV, directional control valve.

Whereas pumps impart energy to liquid only during operation, a pressure tank can capture and store the liquid under pressure for discharge at a later time. It achieves this by compression of gas inside its closed volume. As the liquid is pumped into the pressure tank, the volume occupied by the gas decreases. As per Boyle's law, the pressure exerted by a given mass of an ideal gas is inversely proportional to the volume it occupies. There are different constructions of pressure tanks related to how the liquid and gas are isolated, but all operate according to this principle. These 3 devices require different control strategies to deliver nutrient solutions to nozzles at up to 10 bars of pressure, as shown in Table 4.

With the PD pump setup, the intersection of the pump and system resistance curves is changed by using a VFD (variable frequency drive) to set the pump speed. This translates the pump curve along the  $X$ -axis (flow rate) while minimally affecting the slope. The centrifugal pump setup changes the intersection by using a flow adjustment valve to throttle the discharge. This has the effect of rotating the system resistance curve. The effects of a VFD and flow adjustment valve are shown in Figure 6.

In comparison, determining the operating point of the pressure tank setup is trivial. Unlike the former systems, where characteristic curves must be determined analytically, the pump simply operates in on/off mode with a cut-in and cut-out pressure set by the operating limits of the pressure tank. Although additional solenoid

valves are required downstream of the pressure tank to time and control spray cycles, this helps achieve short spray durations. Given some plant water requirement, shorter frequent sprays can lead to better water utilisation than longer intermittent sprays. Aeroponic irrigation was thought to exist on a continuum with hydroponics, with the complete and constant immersion of roots on one extreme and short, frequent sprays on the other. Solenoid valves offered the possibility of sub-second spray cycles, whereas the same duration for a pump would cause pulsatile outputs and transients in voltage and pressure. For these reasons, a pressure tank paired with a PD pump was chosen to supply the necessary pressures for atomisation.

The second and third requirements were attempted to be satisfied with the arrangement of the remaining parts of the fertiliser dosing unit. The main considerations when designing the arrangement were pipe sizes, relative locations of components, and maintenance/safety devices. Pipe sizes were largely determined by the threaded interfaces of sensors, with 3/4 NPT being the most common thread size. Although pipe sizes could be made smaller or larger independent of the sensor interfaces, this requires using multiple threaded or cemented fittings, which increases the cost, size, and likelihood of leaks. As a 3/4 pipe size was more than sufficient to meet flow rate requirements, it was used throughout the entire unit to simplify fabrication. Locations of components relative to

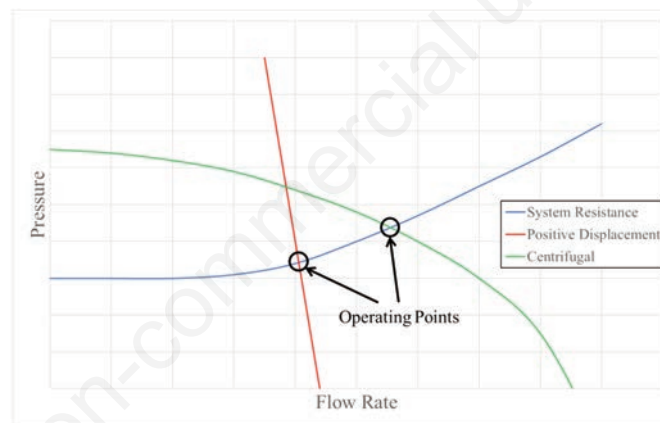


Figure 5. Typical performance curves of PD and centrifugal pumps overlaid on top of a generic system resistance curve.

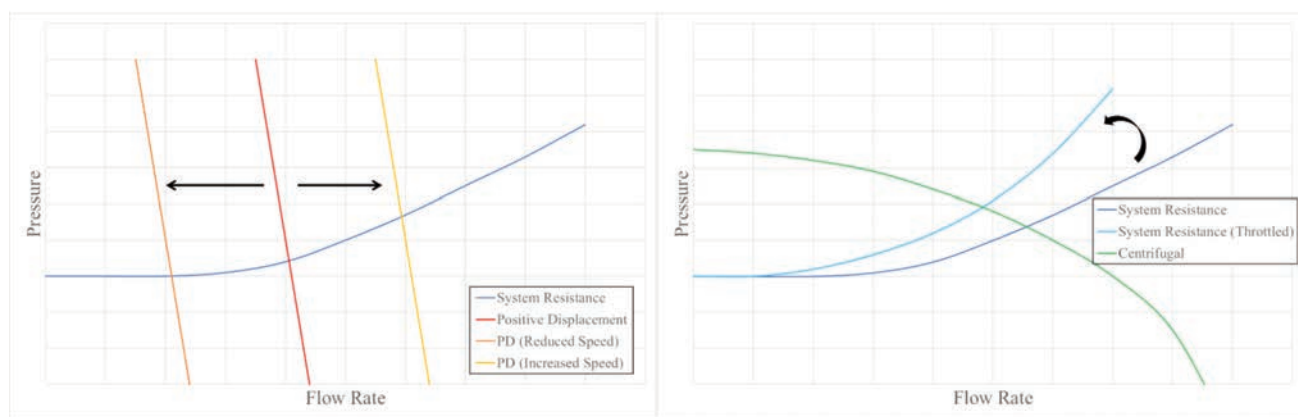


Figure 6. Operating points varied by changing the pump or system resistance curves.

one another were also important to meet design intent. For example, mixers were required downstream of metering pumps, water hammer eliminators were required upstream of solenoid valves, and sensors were needed throughout various sections to monitor and control RO water and nutrient solution. The conductivity and pH sensors also had an orientation requirement, with the preferred installation directing flow straight into the probe. As this was impractical to accommodate all sensors, only the conductivity sensor was installed in this orientation. Maintenance and safety devices were placed in a manner that enabled easy access and increased passive safety. For example, ball valves were placed throughout the unit to allow drainage and isolation of specific zones. In addition, pressure relief valves were placed near the outlet of pumps and pressure tanks. This decreased the severity of failures that could occur in the event that an isolation valve was inadvertently closed or a solenoid valve failed a mid-operation. The full arrangement can be found in Figure 7.

Independent control of nutrient solution concentrations between the 2 root chambers was achieved by having 2 sets of pressure tanks, associated sensors (conductivity, pH, and pressure), and inlet solenoid valves. The concentrated nutrient solution was injected by 2 metering pumps, mixing with the RO stream to create the dilute nutrient solution. The metering pumps were PID controlled with the setpoint determined by the stage of life of the plant and the process value being the difference between the nutrient solution and RO water conductivity sensors. In addition, these sensor pairs were programmed to use the RO water conductivity value as a zero-point offset for the nutrient solution conductivity sensor. This allows the system to account, adjust, and monitor for the conductivity of the inlet water.

### Grow tray and substrate

In aeroponics, plant roots are not fully embedded in any substrate. In fact, the majority of plant roots are suspended in the air. This free suspension allows water droplets to directly contact the plant roots. However, the plant's mass still needs to be supported. This is the primary function of the grow tray and substrate, to hold the plants at a set distance above the nozzle array. In addition, the grow tray and substrate isolate the canopy and root chamber environments, which have very different needs to allow the proper functioning of the shoot and root biomass. The grow tray (*T*), substrate (*S*), and combined (*C*) requirements are:

T1. Support the mass of water-saturated substrate and plants across the entire grow tray with a deflection no greater than 50 mm.

- T2. Have an open area greater than 80% to allow plant roots to go down into the root chamber.
- T3. Resist corrosion from water, inorganic, and organic compounds found in the nutrient solution.

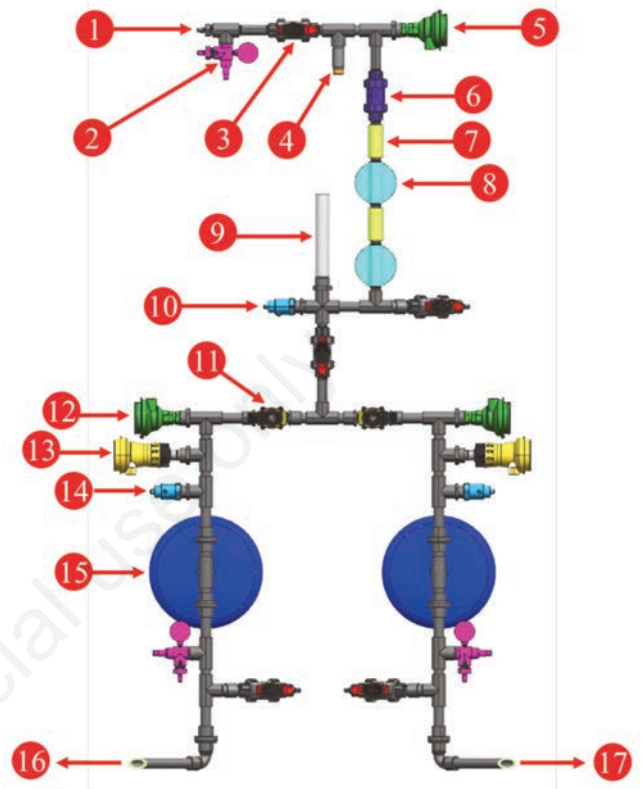


**Figure 7. Fertiliser dosing unit.** 1, system inlet, reverse osmosis water; 2, 3x piston type pressure relief valve; 3, 5x ball type isolation valve; 4, 1x temperature sensor, reverse osmosis water; 5, 1x conductivity sensor, reverse osmosis water; 6, 1x ball type check valve; 7, 2x injection pump fitting; 8, 2x mixer; 9, 1x water hammer eliminator; 10, 1x pressure sensor, positive displacement pump; 11, 2x diaphragm type solenoid valve; 12, 2x conductivity sensor, nutrient solution; 13, 2x pH sensor, nutrient solution; 14, 2x pressure sensor, pressure tank; 15, 2x diaphragm type pressure tank; 16, system outlet, root chamber 1; 17, system outlet, root chamber 2.

**Table 4. Comparison matrix of pumps and pressure tanks for requirement 1.**

	Pump only (PD)	Pump only (centrifugal)	Pressure tank + pump setup
Actively managed components	PD pump with VFD	Centrifugal pump Flow adjustment valve	Pressure tank Pump (either type) Solenoid valve
Nozzle supply pressure control strategy	Speed control of pump using VFD (changes pump curve)	Discharge throttling using flow adjustment valve (changes system resistance curve)	On/off control using solenoid valve downstream of pressure tank
Operating point flexibility	System resistance curves must be modelled to determine operating ranges	System resistance curves must be modelled to determine operating ranges	Operating point can be set to the entire range of pressure tank pressures
Transient response	Poor Pulsatile output Requires electrical snubbers to handle repeated voltage transients	Poor Requires electrical snubbers to handle repeated voltage transients	Good Function of solenoid valve opening and closing time

VFD, variable frequency drive.

- S1. Wick and hold more than 1x material weight in water to facilitate germination.
- S2. Allow root penetration through the material to facilitate vegetative growth.
- S3. Resist decomposition to minimise debris entering the root chamber.
- C1. Non-toxic to humans and plants.
- C2. Minimise light entering the root chamber.

For the grow tray frame and mesh, 4 common materials used in wet environments were considered. They are aluminium, plated carbon steel, stainless steel 304 [SS304 (SS)], and PVC plastic, as shown in Table 5. Both aluminium and carbon steel are incompatible with some chemicals in fertiliser solution. They both have severe reactions with Potassium Chloride, Boric acid, Potassium Hydroxide, and Nitric acid. Therefore, SS and PVC were found to be the most suitable solution.

The first iteration consists of a layer of cloth sewed at two sides to a PVC pipe frame. This iteration is very cheap and easy to assemble; however, as the cloth was not supported, the weight of the absorbed water pulled the cloth down, as shown in Figure 8.

The second iteration added fishing lines tightened across the pipe frame in a grid configuration, as shown in Figure 9. This method is very effective at preventing the burlap from sagging down. However, stretched fishing lines apply forces that collapse the pipe frame inwards. The pipe frame was fixtured to on the racking system as a countermeasure. As the frame cannot be easily detached, harvesting plants required the burlap to be removed, which was cumbersome and difficult to transport. In addition, burlap does not absorb water well, preventing seeds from germinating.

The third iteration utilised stainless steel mesh to support the grow substrate. Furthermore, burlap was no longer used and was replaced by a bamboo-based substrate, as shown in Figure 10. As a result, the grow tray width is reduced from 1.22m to 0.61m. The combination of SS mesh and smaller tray size allows the grow tray

to be easily installed and removed from the growing rack. This ensures that the process of relocating the grow tray between the cleaning station, seeding station, harvesting station, and grow rack is as simple and easy as possible. The mesh is a welded mesh with a 25.4mm×25.4mm grid, and 14-gauge SS wire, resulting in 85% open area. This weldmesh configuration provides sufficient rigidity with a high open area ratio.

The grow tray frame and mesh must support its own weight and approximately 1 kg of damped grow substrate and plant mass. A simple PVC pipe framing and SS mesh easily satisfy the strength and rigidity requirements. The most important requirement is the chemical compatibility of SS and PVC with the fertiliser solution. According to the compatibility chart, PVC has excellent compati-



Figure 8. The first iteration tray sagging, and the second iteration supported using fishing lines.

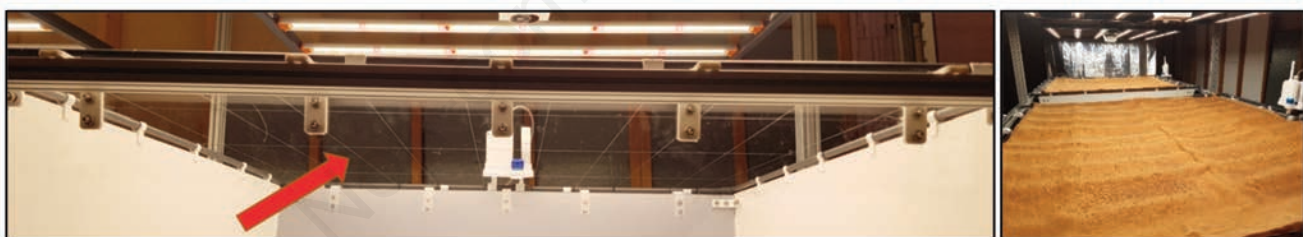


Figure 9. Thin fishing line supporting burlap.

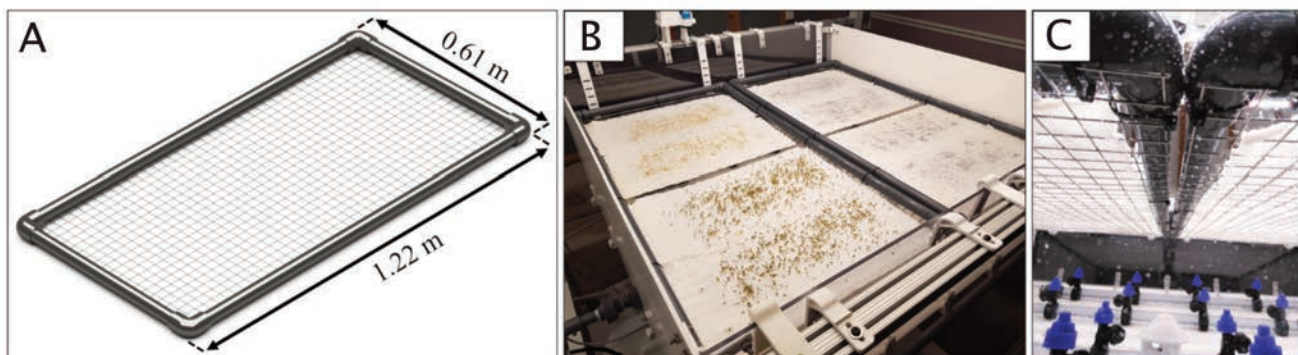


Figure 10. A) Grow tray diagram; B) Top view; C) Bottom view of grow tray and substrate.



bility with all fertiliser chemicals. SS provides adequate compatibility; however, the mesh will come in contact with fertiliser and water much more than the frame, which could lead to the SS mesh degrading much faster than the PVC framing. The compatibility chart does not include copper EDTA, iron DTPA, manganese EDTA, and zinc EDTA. However, these compounds can be categorised as weak acids (Zhao *et al.*, 2015). There is no report on the chemical compatibility of Potassium Phosphate and Sodium Molybdate with SS and PVC. However, visual observations after trials did not indicate any degradation or chemical reaction between the fertiliser and the grow tray.

### Growth monitoring system

Compared to traditional farming, aeroponics is still very much in its infancy. As such, optimal growing strategies are mainly unknown. A lot of research is required to find strategies that maximise yield and achieve good product quality. Although the system is largely automated with respect to recipe control, setpoints of recipes at various plant lifecycles were mostly determined by subjective human observation. To quantitatively analyse the effects of each recipe variable, large amounts of data must be collected quickly and cheaply.

The best yield indicator is to measure plant mass directly. Evaluating plant mass over time provides insight into the growth rate of any particular recipe and allows for the identification of the

most suitable time for harvest, which maximises yield while minimising grow time per batch. However, frequently measuring plant mass is very labour-intensive and risks damaging plants. Instead, it is possible to evaluate plant mass visually. Montagnoli *et al.* (2016) have shown a correlation between the greenness of the growing area and total plant mass. A vision system with cameras that collect colour images is a cheap and effective way of continuously evaluating plant mass over any growing cycle.

In addition to yield, much research was conducted to find the best method of identifying disease using vision information. The best way to identify disease in plants is by visually inspecting their leaves, as leaves often show the earliest symptoms to examine (Nanehkaran *et al.*, 2020). Manual visual inspection is very time-consuming and labour-intensive; therefore, research is extensively done on the best way to automate this process. The most popular approach is using Convolutional Neural Networks. Sladojevic *et al.* (2016) trained their model to differentiate healthy leaves and identify 13 different types of plant diseases with an accuracy of 96.3% on average, as well as distinguished plant leaves from their surroundings. Dhingra *et al.* (2019) used a novel method based on fuzzy logic and neutrosophic logic to identify diseases with an accuracy of 98.4%. Geetharamani and Arun Pandian trained their model to be able to deal with different image conditions, such as different lighting conditions, scalings, and image noises, with an

**Table 5. Chemical compatibility table of various materials considered for the grow tray. The qualitative chemical resistant ratings are, A – excellent, B – good, C – fair, D – severe effect (CP Lab Safety).**

	Aluminium	Carbon steel	Stainless steel 304	Polyvinyl chloride
Potassium Nitrate	B	B	B	A
Ammonium Phosphate	B	D	B	A
Potassium Chloride	D	D	B	A
Boric Acid	D	D	B	A
Calcium Nitrate	B	B	C	A
Magnesium Sulfate	B	B	A	A
Potassium Hydroxide	D	D	B	B
Sodium Hydroxide (0.5-2.0%)	D	D	B	A
Nitric acid (0.5%)	A	D	A	A
Hydrogen Peroxide (15-25%)	A	D	B	A

**Table 6. Hardware used in the aeroponic system.**

Type	Hardware	Manufacturer	Part number	Signal type	Signal range
Input	Pressure sensor	Endress+Hauser	PMP11-CAIL1PFVWJ	Current (mA)	4-20
Input	Electrical conductivity sensor	Signet	3-2850-52-41V	Current (mA)	4-20
Input	pH sensor	Signet	3-2724-00 & 3-2751-2	Current (mA)	4-20
Input	Liquid temperature sensor	Signet	3-2350-3	Current (mA)	4-20
Input	Gas temperature & relative humidity sensor (root)	Vaisala	HMD82	Current (mA)	4-20
Input	Gas temperature & relative humidity sensor (canopy)	Vaisala	HMW88	Current (mA)	4-20
Input	CO2 concentration sensor	Vaisala	GMP252	Current (mA)	4-20
Input	Radiation sensor	Apogee	SQ-514	Current (mA)	4-20
Input	Camera	Reolink	RLC-520	Ethernet IP	N/A
Output	LED drivers (dimming control)	Fluence	SPYDR 2x 47"	Voltage (V)	0-10
Output	Metering pump	Etatron	eOne MF 0710	Current (mA)	4-20
Output	Main pump	Shurflo	8030-863-239	Power Relay	0/1
Output	Solenoid valve	JP Fluid Control	DF-SA034N200F-120AC	Power Relay	0/1

accuracy of 96.46% (Geetharamani and Arun Pandian, 2019). Hassan *et al.* (2021) trained their method to achieve even higher accuracy of between 97.02% and 99.11% with less training time. Nanehkaran used a novel method that utilises hue, saturation, and intensity-based and LAB-based hybrid segmentation algorithms to first segment the images before passing them to a CNN to classify disease (Nanehkaran *et al.*, 2020). Nanehkaran's method was shown to work well with a very complex background. Gajjar *et al.* (2021) method used the advanced Nvidia Jetson TX1, allowing them to achieve high accuracy of 96.88% while identifying a disease from image streaming in real-time. However, all disease detection methods require a large amount of training data. These large datasets can only be obtained after the aeroponics system has been expanded for medium to large-scale production. For the first functional prototype in our study, only a limited dataset can be generated; thus, only greenness algorithms were implemented. Two types of algorithms were tested to segment plant leaves from its surrounding. The first method involves Hue-Saturation-Value (HSV) masking by setting lower and upper threshold values. For example, if a pixel has a hue between 49.4° and 115.5°, saturation between 20% and 100%, and value between 20% and 100%, then that pixel is classified as a leaf. The lower limit colour has a hex code of #333129, and the upper limit colour hex code is #1AFF00.

The second method involves a decision tree-based segmentation model called plant canopy coverage (PCC) masking. The open-source tool EasyPCC was used to implement PCC plant leaves identification (Guo *et al.*, 2017). With both methods, the pixel coordinate identified as plant leaves will take on the binary value 1 (white), and every else will take on the value 0 (black), as shown in Appendix Figure 3.

The cameras are controlled by Python-based microservices running on a Raspberry Pi server. The camera microservice takes a screen capture of the video feed once every 15 minutes. The image is immediately evaluated for its greenness and then saved to the Pi's file system. The summarised data about the images, including the file directory, camera IP address, timestamp, and greenness, is written to a SQL database. Price loss coverage (PLC) is used to control all field devices listed in Table 6. As with the camera, the PLC microservice reads the states of various input, output, and user-defined variables (tags) and logs it into a SQL database (Appendix Figure 4). The logging logic for the PLC was dependent on the nature of events being monitored or controlled. For example, the values of digital IO (binary) were only logged upon change. All analogue IO (continuous) values were logged at varying frequencies.

A Reolink RLC 520 was chosen as the camera (Appendix Figure 5). It is IP66 waterproof and can withstand the high humidity environment above the grow zone. In addition, it has IR vision to observe during the night cycle. One downside of the RLC 520 is its limited field of view of 80° horizontal and 58° vertical. Aeroponics is typically implemented in horizontal plane vertical farms, so minimising the space between each level is important to maximise the number of grow zones possible in height-limited facility. However, this small clearance limits the capture area when the camera is mounted on the light array, as shown in Appendix Figure 6. A multiple stationary camera setup and a single mobile camera platform were considered but were deemed to be unnecessary for the prototype, as the value of a computer vision system had yet to be validated.

## Results and Discussion

### Atomisation

Spray uniformity was validated using rolls of paper as a simulated growing plane. Using semi-absorbent paper, the spray pattern could be visualised before the paper became saturated. These tests identified the largest oversight in the design of the atomisation system. The nozzle sprays did not have a sufficient vertical throw to reach the uppermost grow tray plane, as shown in Appendix Figure 7. The grow trays are height adjustable, at 5 increments between 127 mm to 254 mm above the outer nozzle tips. The left picture in Appendix Figure 8 shows the spray pattern at the lowest plane, while the right picture shows the spray pattern at the middle plane. A simultaneous 10s spray at 80 psi from both counter parallel nozzle arrays was used for these images.

Due to this error, only the lowest growing plane could be used throughout the grow trials. The consequences were numerous dry spots, as the design intent required overlapping spray patterns to cover the growing plane uniformly. Nonetheless, the geometric spray model was modified for comparison with physical observations made at the lowest height, as shown in Appendix Figure 9.

It is difficult to make a quantitative observation due to the crude nature of visualising using paper. Additionally, the patterns of individual nozzles are difficult to parse out as there is a small degree of overlap. However, two observations can be made. The first is the total length and width of the array pattern measured on paper was 965.2 mm×863.6, whereas the model showed 924.6 mm×906.78 mm. This suggests some validity in using a simplified geometric spray model to optimise spray uniformity. The second is that there is greater saturation on the outboard side of the hollow cone spray. This is likely due to the shorter spray distance on this side of the cone, resulting in a greater droplet flux.

### Fertiliser dosing unit

Requirements 2 and 3 were unsatisfied with this process arrangement due to poor PID performance. Although the lifecycle of the plant controls the setpoint, the actual input into the PID controller involves a dilution/concentration equation. This is because the pressure tank operates between partial charge and discharge levels, so additional volumes of nutrient solution will dilute or concentrate the initial solution. The equation is as follows.

$$c_f V_f = c_i V_i + c_a V_a \quad (1)$$

where  $c_f$  is the final concentration (based on the lifecycle of the plant),  $V_f$  is the final volume (pressure tank volume at cut-out pressure),  $c_i$  is the initial concentration (pressure tank conductivity sensor reading),  $V_i$  is the initial volume (pressure tank volume at cut-in pressure),  $c_a$  is the additional concentration (set point for PID controller), and  $V_a$  is the additional volume ( $V_f - V_i$ ).

Re-arranging this equation to solve for  $c_a$  yields,

$$c_a = \frac{c_f V_f - c_i V_i}{V_a} \quad (2)$$

From Eq. (2), one can note that increasing the additional volume decreases the additional concentration. This reduces the error value that the PID controller must correct for and increases the time that the PID controller has to reach a steady state as the PID pump must run for a longer time. Decreasing the final concentra-

tion also has the same effect on the error value. Substitution of this equation with one set of operational values yields,

$$c_a = \frac{(0.5 \frac{dS}{m})(9501 \text{ mL}) - (0 \frac{dS}{m})(6334 \text{ mL})}{(3167 \text{ mL})} = 1.5 \frac{dS}{m} \quad (3)$$

In other words, to increase the concentration of the pressure tank from 0 to  $0.5 \frac{dS}{m}$ , the set point of the PID controller must be

$1.5 \frac{dS}{m}$ . However, the effect of the existing volume upstream of the solenoid valves was not accounted for during design. This volume must be displaced before the newly mixed nutrient solution enters the pressure tank, as shown in Appendix Figure 10. This ultimately reduces the volume and time that the PID controller has to adjust the concentration.

A single mixer has an approximate volume of 1733 mL, meaning that displacement of 2 mixers alone would reach the cut-out pressure of 80 psi. Increasing the drawdown volume of the pressure tank was explored but was limited in effectiveness due to the sensor and pressure tank's maximum and minimum pressure envelopes, respectively. Although the nutrient concentration was slowly increased during trials, it was achieved with no real accuracy nor independence between the 2 pressure tanks. Other unforeseen problems include incomplete isolation of zones due to bypass from the diaphragm-type solenoid valves and ball-type check valves. To address these limitations, the fertiliser mixing unit and the pressure tanks are being decoupled in the next iteration of the grow unit. In addition, a reservoir is placed between the pressure tanks and mixing unit to act as a process buffer.

### Grow tray and substrate

The third iteration solved some challenges; however, using organic substrate poses another issue regarding contamination. The substrate appears to be easily infected with fungi during the grow trials. To prevent this fungi contamination in the grow zone, a different grow substrate material has to be researched. However, grow substrates with high durability leads to difficult end-of-life disposal. Therefore, trade-off research between environmentally friendly disposal *versus* durability and cleanliness needs to be conducted in the future.

### Growth monitoring system

Greenness data from grow trials utilised the data collection scheme particularly well. In a 30-day grow trial of rocket, a nozzle clogging problem occurred and effectively killed off a small section of plants. This event can be seen in Appendix Figure 11A and B. Approximately 21 days into the trial (point a), the percentage of greenness stopped following a smooth trend and slowed down. On the 22nd day (point b), the nozzle was fully clogged and discharged no water. This caused a dry-out and killed some plants. Again, a large drop in the percentage of greenness can be seen. This experiment has shown that it is possible to detect the growing issue with the vision system alone.

The graph comprises approximately 1500 data points; each data point is the percentage greenness of the taken image at a particular point in time. The graph presents the night cycle gap when the environment is dark, and therefore no colour can be captured. Each day cycle also appears to increase and then decrease. This is caused by the plant's circadian rhythms, where plants expand and reach out to absorb more light in the middle of the day, then col-

lapse back when night comes. EasyPCC algorithm is capable of separating plant leaves pixels from their background. HSV is a much simpler algorithm, but it has proven to be as capable as EasyPCC. As shown in Appendix Figure 11, both HSV and EasyPCC method provides very similar greenness evaluation.

## Conclusions

This paper explored the considerations and trade-offs involved in designing an aeroponic cultivation unit. Atomisation was achieved using pressure swirl atomisers due to their simplicity of operation. To achieve the supply pressures needed for effective atomisation, the fertiliser dosing unit mixed and stored nutrient solution inside a pressure tank on an on-demand basis. However, the unit configuration did not allow for accurate and independent control of nutrient concentration between the 2 zones. The developed grow tray and substrate were found to be suitable for both germination and vegetative growth but also allowed significant algae and fungi contamination to occur. The camera-based EasyPCC and HSV algorithms and the camera microservice were developed to monitor the leafy green's growth.

The main objective of this aeroponic cultivation unit was to create a quantitative growth model for various species of leafy greens. This quantitative model would then be used to answer whether aeroponics truly leads to greater productivity than conventional hydroponic systems. Furthermore, does greater control of the root zone environment actually matter, given the trade-off of additional complexity and capital expense? Unfortunately, this question could not be answered with the first prototype. However, this study presents the development process of an aeroponic system for leafy green cultivation and details the challenges in the design and engineering of this system in terms of atomisation, fertiliser dosing, grow tray/substrate, and growth monitoring as a key component. Therefore, this technical exercise, specialising in equipment development and testing will contribute to reducing the time and effort of other groups attempting to design an aeroponic system by sharing the thought process behind the design and learning lessons from trials.

## References

- Aluminum chemical compatibility. CP Lab Safety. Available from: <https://www.calpaclab.com/aluminum-chemical-compatibility-chart>.
- Benke K., Tomkins B. 2017. Future food-production systems: vertical farming and controlled-environment agriculture. *Sustain.: Sci. Pract. Policy*. 13:13-26.
- BETE 1218USA catalog. BETE. 2019. Available from: [https://www.bete.com/PDFs/BETE\\_1218USA\\_Catalog.pdf](https://www.bete.com/PDFs/BETE_1218USA_Catalog.pdf)
- Carbon steel chemical compatibility chart. CP Lab Safety. Available from: <https://www.calpaclab.com/carbon-steel-chemical-compatibility-chart>.
- Catalog 51A. TeeJet. 2014. Available from: [https://www.teejet.com/CMSImages/TEEJET/documents/catalogs/cat51a\\_us.pdf](https://www.teejet.com/CMSImages/TEEJET/documents/catalogs/cat51a_us.pdf).
- Clawson J., Hoehn A., Stodieck L., Todd P., Stoner R. 2000. Re-examining aeroponics for spaceflight plant growth. SAE. Technical. Papers.
- Colmer T. 2003. Long-distance transport of gases in plants: a perspective on internal aeration and radial oxygen loss from roots. *Plant. Cell. Environ.* 26:17-36.

- Despommier D. 2011. The vertical farm: controlled environment agriculture carried out in tall buildings would create greater food safety and security for large urban populations. *JVL*. 6:233-6.
- Dhingra G., Kumar V., Joshi H.D. 2019. A novel computer vision based neutrosophic approach for leaf disease identification and classification. *Measurement*. 135:782-94.
- Eldridge B., Manzoni L., Graham C., Rodgers B., Farmer J., Dodd A. 2020. Getting to the roots of aeroponic indoor farming. *New Phytol.* 228:1183-92.
- Gajjar R., Gajjar N., Thakor V.J., Patel N.P., and Ruparelia S. 2021. Real-time detection and identification of plant leaf diseases using convolutional neural networks on an embedded platform. *Visual. Comput.* 38:2923-38.
- Geetharamani G., Arun Pandian J. 2019. Identification of plant leaf diseases using a nine-layer deep convolutional neural network. *Comput. Elect. Eng.* 76:323-38.
- Guo W., Zheng B., Duan, T., Fukatsu T., Chapman S., Ninomiya S. 2017. EasyPCC: benchmark datasets and tools for high-throughput measurement of the plant canopy coverage ratio under field conditions. *Sensors*. 17:798.
- Hassan SK.M., Maji A.K., Jasiński M., Leonowicz Z., Jasińska E. 2021. Identification of plant-leaf diseases using CNN and transfer-learning approach. *Electronics*. 10:1388.
- Kozai. T. 2018. *Smart plant factory: the next generation indoor vertical farms*. Singapore: Springer Singapore.
- Lakhiar I.A., Gao J., Syed T.N, Chandio F.A., Buttar N.A. 2018. Modern plant cultivation technologies in agriculture under controlled environment: a review on aeroponics. *J. Plant. Interact.* 13:338-52.
- Laugerette T., Stöckel F. 2016. From Agriculture to AgTech - an industry transformed beyond molecules and chemicals. Deloitte, 8. Available from: <https://www2.deloitte.com/content/dam/Deloitte/de/Documents/consumer-industrial-products/Deloitte-Transformation-from-Agriculture-to-AgTech-2016.pdf>
- Lefebvre A., McDonell, V. 2017. *Atomization and sprays*, Second edition. ed. (Combustion: an international series). Boca Raton, FL: Taylor & Francis, CRC Press.
- Li Q., Li X., Tang B., Gu M. 2018. Growth responses and root characteristics of lettuce grown in aeroponics, hydroponics, and substrate culture. *Horticulturae*. 4:35.
- Montagnoli A., Terzaghi M., Fulgaro N., Stoew B., Wipenmyr J., Ilver D., Rusu C., Scippa, G.S., Chiatante, D. 2016. Non-destructive phenotypic analysis of early stage tree seedling growth using an automated stereovision imaging method. *Front. Plant. Sci.* 7:1644.
- Nanehkaran Y.A., Zhang D., Chen J., Tian Y., Al-Nabhan N. 2020. Recognition of plant leaf diseases based on computer vision. *J AMB INTEL HUM COMP J. Amb. Intel. Hum. Comp.* 1-18
- Pittman R. 2016. *Regulation of tissue oxygenation*, 2nd ed. (Colloquium series on integrated systems physiology, # 65). San Rafael, CA: Morgan and Claypool Life Sciences.
- Pumps, spray nozzles, and accessories. Pentair. 2018. Available from: <https://www.pentair.com/content/dam/extranet/flow/catalogs/HYP01-Catalog.pdf>.
- PVC chemical compatibility. CP Lab Safety. Available from: <https://www.calpaclab.com/pvc-polyvinyl-chloride-chemical-compatibility-chart>.
- Sladojevic S., Arsenovic M., Anderla A., Culibrk D., Stefanovic D. 2016. Deep neural networks based recognition of plant diseases by leaf image classification. *Comput. Intel. Neurosc.* 2016:3289801-11.
- Specht K., Siebert R., Hartmann I., Freisinger U.B., Sawicka M., Werner A., Thomaier S., Henckel D., Walk H., Dierich A. 2014. Urban agriculture of the future: an overview of sustainability aspects of food production in and on buildings. *Agr. Hum. Values.* 31:33-51.
- Stainless steel chemical compatibility chart. CP Lab Safety. Available from: <https://www.calpaclab.com/stainless-steel-chemical-compatibility-chart>.
- Thakur K., Partap M., Kumar D., Warghat A.R. 2019. Enhancement of picrosides content in *Picrorhiza kurroa* Royle ex Benth. mediated through nutrient feeding approach under aeroponic and hydroponic system. *Ind. Crop. Prod.* 133:160-7.
- Wyslouzil B.E., Whipple M., Chatterjee C., Walcerz, D.B., Weathers P.J., Hart D.P. 1997. Mist deposition onto hairy root cultures: aerosol modeling and experiments. *Biotechnol. Progr.* 13:185-94.
- Zhao F., Repo E., Yin D., Meng Y., Jafari S., Sillanpää M. 2015. EDTA-Cross-Linked  $\beta$ -Cyclodextrin: an environmentally friendly bifunctional adsorbent for simultaneous adsorption of metals and cationic dyes. *Environ. Sci. Technol.* 49: 10570-80.